

---

This is an electronic reprint of the original article.  
This reprint may differ from the original in pagination and typographic detail.

Seisko, Sipi; Lampinen, Matti; Aromaa, Jari; Laari, Arto; Koironen, Tuomas; Lundström, Mari  
**Kinetics and mechanisms of gold dissolution by ferric chloride leaching**

*Published in:*  
Minerals Engineering

*DOI:*  
[10.1016/j.mineng.2017.10.017](https://doi.org/10.1016/j.mineng.2017.10.017)

Published: 01/01/2018

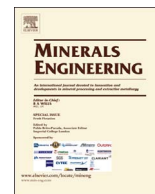
*Document Version*  
Publisher's PDF, also known as Version of record

*Published under the following license:*  
CC BY-NC-ND

*Please cite the original version:*  
Seisko, S., Lampinen, M., Aromaa, J., Laari, A., Koironen, T., & Lundström, M. (2018). Kinetics and mechanisms of gold dissolution by ferric chloride leaching. *Minerals Engineering*, 115, 131-141.  
<https://doi.org/10.1016/j.mineng.2017.10.017>

---

This material is protected by copyright and other intellectual property rights, and duplication or sale of all or part of any of the repository collections is not permitted, except that material may be duplicated by you for your research use or educational purposes in electronic or print form. You must obtain permission for any other use. Electronic or print copies may not be offered, whether for sale or otherwise to anyone who is not an authorised user.



# Kinetics and mechanisms of gold dissolution by ferric chloride leaching



Sipi Seisko<sup>a</sup>, Matti Lampinen<sup>b</sup>, Jari Aromaa<sup>a</sup>, Arto Laari<sup>b</sup>, Tuomas Koironen<sup>b</sup>, Mari Lundström<sup>a,\*</sup>

<sup>a</sup> Aalto University, School of Chemical Engineering, Department of Chemical and Metallurgical Engineering, P.O. Box 16200, 00076 Aalto, Helsinki, Finland

<sup>b</sup> Lappeenranta University of Technology, School of Engineering Science, P.O. Box 20, FI-53851 Lappeenranta, Finland

## ARTICLE INFO

### Keywords:

Gold leaching  
RDE  
Oxidant concentration  
Modeling  
Markov chain Monte Carlo

## ABSTRACT

Gold dissolution was investigated in ferric chloride solution, being one alternative cyanide-free leaching media of increasing interest. The effect of process variables ( $[Fe^{3+}] = 0.02\text{--}1.0\text{ M}$ ,  $[Cl^-] = 2\text{--}5\text{ M}$ ,  $pH = 0\text{--}1.0$ ,  $T = 25\text{--}95\text{ }^\circ\text{C}$ ) on reaction mechanism and kinetics were studied electrochemically using rotating disk electrode with  $\omega_{cyc} = 100\text{--}2500\text{ RPM}$  and Tafel method. The highest gold dissolution rate ( $7.3 \cdot 10^{-4}\text{ mol m}^{-2}\text{ s}^{-1}$ ) was achieved at  $95\text{ }^\circ\text{C}$  with  $[Fe^{3+}] = 0.5\text{ M}$ ,  $[Cl^-] = 4\text{ M}$ ,  $pH = 1.0$  and  $\omega_{cyc} = 2500\text{ RPM}$ . Increase in gold dissolution rate was observed with increase in temperature, ferric ion concentration and chloride concentration, but gold dissolution rate did not have a clear dependency on pH. Redox potential was found to vary between 636 and 741 mV vs. SCE during experiments. According to the calculated equilibrium and measured open circuit potentials, gold was suggested to dissolve as aurous ion  $Au^+$  and form  $AuCl_2^-$ , rather than auric ion  $Au^{3+}$  and form  $AuCl_4^-$ . Further, it is suggested that  $AuCl_2^-$  does not oxidize to  $AuCl_4^-$  under the investigated conditions. Levich plot and the calculated activation energies suggested that gold dissolution was limited by mass and electron transfer. According to a mechanistic kinetic model developed in the current work, intrinsic surface reaction mainly controls gold dissolution, especially at higher rotational speeds ( $> 1000\text{ RPM}$ ). Uncertainties in the model parameters of the mechanistic kinetic model were studied with Markov chain Monte Carlo methods.

## 1. Introduction

Cyanide leaching is the predominant method used in gold production from primary raw materials (Marsden and House, 2006) regardless of the toxic nature of the chemical posing a significant health threat if exposed to the ecological entities (Hilson and Monhemius, 2006). Since the Baia Mare disaster in Romania in 2000, the use of cyanide has been the subject of international concern (UNEP/OCHA, 2000). Moreover, several countries have started to ban cyanidation via legislation, e.g., Costa Rica, many states of the USA and provinces within Argentina (Laitos, 2012). Therefore, alternative solutions, such as thiourea, thio-sulphate, oil-coal agglomerates as well as halides have been proposed to replace cyanide (Adams, 2016; Aromaa et al., 2014; Aylmore, 2005; Hilson and Monhemius, 2006; Lampinen et al., 2015a).

Halide gases ( $Cl_2$  and  $Br_2$ ) have been industrially used since the 19th century in gold ore leaching due to their oxidative nature and ability for gold complexation by  $Cl^-/Br^-$  ions in solution originating from  $Cl_2$  and  $Br_2$  gases (Kirke Rose, 1898). The disadvantage in the use of halide gases is that they are expensive, strongly corrosive, and requires high focus on safety and storing during operation. In addition, the use of halide gases can induce high redox potentials that result in gold passivation (Abe and Hosaka, 2010).

Chloride leaching provides major advantages for hydrometallurgical processing, as it supports high metal solubility, enhanced redox potentials and high leaching rates (Liddicoat and Dreisinger, 2007). According to Abe and Hosaka (2010), ferric ion can be an effective oxidant in chloride media for gold leaching, gold dissolution occurring at lower redox potentials compared to chlorine and aqua regia leaching. A redox potential of  $\geq 480\text{ mV}$  (vs. Ag/AgCl) is required in ferric chloride leaching compared with typical redox potentials of  $\geq 778\text{ mV}$  (vs. Ag/AgCl) in chlorine/bromine gas leaching (Abe and Hosaka, 2010). Ferric and cupric chloride leaching can have advantage over cyanidation being capable for refractory gold mineral leaching, without pre-treatment like pressure oxidation or roasting (Angelidis et al., 1993; Marsden and House, 2006; Lundström et al., 2014; van Meersbergen et al., 1993). According to Aylmore (2005), 4% of publications for alternative lixivants to cyanide in gold leaching were under category oxidative chloride processes including aqua regia and acid ferric chloride. Further, some patents have been subjected for ferric chlorides for gold leaching (Abe and Hosaka, 2010; Lundström et al., 2016).

Gold can be present in aqueous chloride solution as either in monovalent aurous form  $Au^+$  or trivalent auric form  $Au^{3+}$  (Marsden and House, 2006). Putnam (1944) suggested that the dissolution of gold proceeds in two steps: formation of intermediate  $AuCl_2^-$  occurs by

\* Corresponding author.

E-mail address: [mari.lundstrom@aalto.fi](mailto:mari.lundstrom@aalto.fi) (M. Lundström).

## Nomenclature

### List of symbols

$A$	area of the electrode ( $\text{mm}^2$ or $\text{cm}^2$ )
$b_a$	Tafel slope coefficient of the anodic side ( $\text{mV decade}^{-1}$ )
$b_c$	Tafel slope coefficient of the cathodic side ( $\text{mV decade}^{-1}$ )
$B$	systematic coefficient (mV)
$C_O^*$	concentration of oxidant in bulk solution ( $\text{mol cm}^{-3}$ )
$c_{\text{Cl}^-,\text{blk}}$	concentration of the chloride ion at liquid bulk phase ( $\text{mol L}^{-1}$ )
$c_{\text{Fe}^{3+},s}$	concentration of the oxidant at the disc surface ( $\text{mol L}^{-1}$ )
$d$	rotating disc diameter (m)
$D$	diffusion coefficient ( $\text{m}^2 \text{s}^{-1}$ )
$D_O$	diffusion coefficient of oxidant ( $\text{cm}^2 \text{s}^{-1}$ )
$E_a$	activation energy ( $\text{J mol}^{-1}$ )
$E^0$	standard potential (V)
$F$	Faraday's constant ( $\text{C mol}^{-1}$ )
$i$	sum of the currents ( $\text{mA cm}^{-2}$ )
$i_K$	electron transfer-limited current ( $\text{mA cm}^{-2}$ )
$i_{\text{lim},c}$	diffusion-limited cathodic current ( $\text{mA cm}^{-2}$ )
$j_{\text{corr}}$	corrosion current density ( $\text{A cm}^{-2}$ )
$k$	reaction rate constant
$k_L$	mass transfer coefficient through the boundary layer

$k_{\text{mean}}$	rate constant at the reference temperature ( $(\text{m}^3 \text{kmol}^{-1})^{n-1} \text{m s}^{-1}$ )
$n$	reaction order for the oxidant
$\omega_{\text{rad}}$	angular speed of the electrode ( $\text{rad s}^{-1}$ )
$\omega_{\text{cyc}}$	rotational speed of the electrode (RPM)
$n_{\text{Fe}^{3+}}$	mass transfer of the $\text{Fe}^{3+}$ through the boundary layer ( $\text{mol m}^{-2} \text{s}^{-1}$ )
$r_s$	surface reaction rate ( $\text{mol m}^{-2} \text{s}^{-1}$ )
$R$	gas constant ( $\text{J mol}^{-1} \text{K}^{-1}$ )
$Re$	Reynolds number
$R_p$	linear polarization resistance (LPR) ( $\Omega \text{cm}^2$ )
$Sc$	Schmidt number
$Sh$	Sherwood number
$T$	temperature (K)
$T_{\text{mean}}$	reference temperature (K)
$z$	the number of transferred electrons during reaction

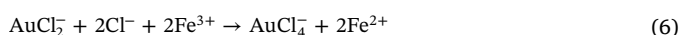
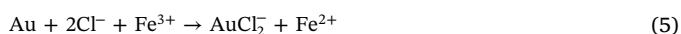
### Greek symbols

$\gamma$	stoichiometric coefficient of $\text{Fe}^{3+}$ to oxidize 1 mol of gold
$\mu$	solution dynamic viscosity (mPa s)
$\nu$	solution kinematic viscosity ( $\text{cm}^2 \text{s}^{-1}$ )

anodic reaction at the gold surface, Eq. (1), after which AuCl forms a more stable complex  $\text{AuCl}_2^-$ , Eq. (2).  $\text{AuCl}_2^-$  is the prevailing species at oxidation potentials  $< 1.2$  V vs. Standard Hydrogen Electrode (SHE), whereas oxidation further into  $\text{AuCl}_4^-$  can occur at oxidation potentials  $> 1.2$  V vs. SHE (0.956 V vs. SCE), Eq. (3) (Nicol, 1980). According to Diaz et al. (1993), gold dissolves as an  $\text{AuCl}_2^-$  complex with an oxidation state +1, when the potential is 0.8 V vs. Saturated Calomel Electrode (SCE) (1.044 V vs. SHE) and also as  $\text{AuCl}_4^-$  complex with oxidation state +3 at higher potentials. Frankenthal and Siconolfi (1982) also suggested that gold dissolves as aurous ions  $\text{Au}^+$ , when the potential is below 0.8 V vs. SCE, but as auric  $\text{Au}^{3+}$  ions, when the potential is above 1.1 V vs. SCE. Furthermore, Diaz et al. (1993) proposed that  $\text{AuCl}_2^-$  complexes can oxidize into  $\text{AuCl}_4^-$  complexes by a very slow disproportionation reaction (Eq. (4)).



The net reaction of gold dissolution in ferric chloride solution is described in Eq. (5) according to the gold dissolution steps by Putnam (1944) and Liu and Nicol (2002). Furthermore, the net reaction of  $\text{AuCl}_2^-$  oxidizing into  $\text{AuCl}_4^-$  ions is presented in Eq. (6) (Liu and Nicol, 2002). The regeneration of ferrous ions back to ferric ions or ferric chloride complexes can be achieved by oxygen purging, Eq. (7) (Abe and Hosaka, 2010; Liu and Nicol, 2002; Lu and Dreisinger, 2013; Senanayake, 2004). This reuse of oxidant via regeneration is a major advantage in chloride leaching (Abe and Hosaka, 2010).



Ferric ion can exist in chloride solutions in ionic form, but also with increasing chloride concentration as chloride complexes such as  $\text{FeCl}_2^+$ ,  $\text{FeCl}_2^+$  and  $\text{FeCl}_3(\text{aq})$  (Muir, 2002). Further, Strahm et al. (1979) demonstrated that the amount of  $\text{Fe}^{3+}$  species reduced and the

amount of  $\text{FeCl}_2^+$ ,  $\text{FeCl}_2^+$ ,  $\text{Fe}(\text{H}_2\text{O})\text{Cl}_2^+$  as well as  $\text{FeCl}_3(\text{aq})$  species increased, when chloride concentration increased. Their results suggested that  $\text{Fe}^{3+}$  species are predominant with chloride concentration from 0 to 2 M,  $\text{FeCl}_2^+$  from 2 to 5 M and  $\text{FeCl}_3(\text{aq})$  above 5 M (Strahm et al., 1979). According to O'Melia (1978), ferric ions occur predominantly as chloro complexes, when ferric ion concentration is between 0 and 1 M and pH below 2. In the temperature range 0–100 °C, the equilibrium constant ( $K$ ) for  $\text{FeCl}_2^+$  formation is 29–72 and for  $\text{FeCl}_2^+$  formation  $K = 10^{13}$ – $10^{15}$  (HSC 8.1, 2015). This suggests that as long as enough chloride ions are present the ferric iron will be in chloride complexes.

Many process variables, such as temperature, ferric iron and chloride concentration as well as pH, can affect the dissolution of gold. According to Liu and Nicol (2002) increase in temperature, chloride concentration and ferric to ferrous ratio improves gold dissolution in ferric chloride pressure leaching. Different temperature ranges have been investigated and/or suggested for ferric chloride leaching:  $\leq 85$  °C (Abe and Hosaka, 2010), 90–100 °C (Lundström et al., 2016) and 25–200 °C in pressurized conditions (Liu and Nicol, 2002). Abe and Hosaka (2010) suggested the optimal ferric ion concentration in chloride leaching being 0.01–0.26 g  $\text{L}^{-1}$  (0.0002–0.0047 M), whereas Lundström et al. (2016) suggested ferric ion concentration of 9–20 g  $\text{L}^{-1}$  (0.16–0.36 M) being advantageous. In chloride solutions, the oxidation of base metal sulfides generally results in elemental sulfur formation at pH values close to 1.5 (Lundström et al., 2008; Lundström et al., 2009). This may result in the formation of layers that prevent gold dissolution (Abe and Hosaka, 2010).

von Bonsdorff (2006) used a maximum chloride concentration of 5.0 M for gold leaching, while Lundström et al. (2016) stated that the chloride concentration in ferric chloride leaching process can be below 120 g  $\text{L}^{-1}$  ( $< 3.39$  M). However, it must be noted that the optimal chloride concentration depends on raw material, with increasing impurities present, higher amount of chlorides are complexed with base and precious metals dissolved into the solution.

Investigations by Abe and Hosaka (2010), also showed that pH lower than 1.9 favors soluble iron during ferric chloride leaching, whereas at higher pH iron precipitates as hydroxides. The solubility of iron increases with decreasing pH, and it has been stated that the pH must be  $\leq 1.9$  in order to ensure that the iron is at least partially soluble

and can act as oxidant in ferric chloride leaching of gold (Abe and Hosaka, 2010). Moreover, it has been suggested that pH in ferric chloride leaching should be between 0.5 and 1.9 as the gold dissolution rate decreases at pH values below 0.5 (Abe and Hosaka, 2010). According to Lundström et al. (2016), the preferred pH in ferric chloride leaching is between 1 and 1.5.

It has been suggested previously that the presence of HCl decreases the solubility of sodium chloride (Potter and Clyne, 1980), whereas increase in temperature increases the solubility of sodium chloride. In this work, the concentrations of HCl used for pH adjustment were low (max 0.28 M (10.2 g L<sup>-1</sup>)) and as a result did not have an effect on the solubility of sodium chloride in the investigated system.

Dissolution of gold can be limited by mass transfer, electron transfer or a combination of these referred to as mixed control. It has been stated that for a diffusion controlled reaction, the values of activation energies are below 21 kJ mol<sup>-1</sup> whereas for reactions controlled by electron transfer, the values of activation energies in the range of 40–100 kJ mol<sup>-1</sup> (Peters, 1973). Furthermore, when the effect of diffusion is no longer a rate limiting step, other phenomena will replace it.

Recently, Lampinen et al., (2017) investigated the mechanism and kinetics of cupric chloride leaching of gold. In the case of ferric chloride leaching of gold, very limited amount of work has been published at atmospheric conditions. Therefore, electrochemical methods such as linear polarization resistance (LPR) using rotating disc electrode (RDE) and polarization measurements (Tafel method) were performed for pure gold in ferric chloride media. The target of this work was to reveal the effect of parameters such as temperature, ferric ion concentration, chloride concentration, and pH on gold dissolution. In addition, the reaction mechanism and rate-limiting step were clarified by linearization approach as well as by developing a mechanistic model. The developed mechanistic model allows to observe the role of intrinsic surface reaction and the mass transfer limitations in gold dissolution reaction. Furthermore, the reliability of the parameters in mechanistic model were studied thoroughly with Markov chain Monte Carlo (MCMC) methods.

## 2. Experiments

### 2.1. Experimental set-up and materials used

RDE measurements were performed in a water-jacketed three electrode cell with a volume of 200 ml, heated by water bath (Lauda M3). The solution volume was 110 ml. The working electrode was 99.99% pure gold RDE ( $d = 5$  mm,  $A = 19.6$  mm<sup>2</sup>) covered in a polytetrafluoroethylene (PTFE) sheath (Pine Research Instrumentation Inc.), counter electrode platinum plate ( $A = 7.1$  cm<sup>2</sup>) and reference electrode Ag/AgCl (SI Analytics) with a potential of 197 mV vs. SHE (Bard and Faulkner, 1980). For the polarization measurements, stationary gold wire (Premion®, purity of 99.999%,  $A = 1.6$ – $2.8$  mm<sup>2</sup>) was used as the working electrode. The gold electrode was thoroughly cleaned with ethanol between every experiment. The chemicals used in the experiments were NaCl (VWR Chemicals, technical grade), FeCl<sub>3</sub> (Merck Millipore, ≥ 98%), HCl (Merck KGaA, Ph. Eur. grade) and NaOH (Sigma-Aldrich, reagent grade).

### 2.2. Parameters investigated

The effect of temperature on gold dissolution was studied at 25–95 °C. The effect of mass transfer was investigated at all temperatures using RDE with 100–2500 RPM in order to determine the rate limiting step. The oxidant (Fe<sup>3+</sup>) concentrations investigated were 0.02, 0.1, 0.25, 0.5, 0.75 and 1.0 M as well as chloride concentrations of 2, 3, 4 and 5 M. Based on literature, pH values 0, 0.5 and 1.0 were investigated, with pH adjusted by HCl (4 M) or NaOH (2 M). Additionally, pH of 1.5 was tested at 95 °C,  $[Fe^{3+}] = 0.1$  M and  $[Cl^-] = 3$  M, however, the iron started to precipitate.

### 2.3. Electrochemical methods and determination of rate limiting step

RDE measurements were performed with an ACM Instrument Gill AC potentiostat using linear polarization resistance sweep by Gill AC Sequencer software (from -10 to 10 mV vs. open circuit potential (OCP), sweep rate of 10 mV min<sup>-1</sup>). Three parallel measurements were performed for each experiment and their average value used to determine the gold dissolution rate. LPR ( $R_p$ ) was determined from the slope of the potential-current density diagram,  $R_p$  being inversely proportional to the dissolution current density ( $j_{corr}$  (mA cm<sup>-2</sup>)), Eq. (8) (Duranceau et al., 2004).

$$j_{corr} = \frac{b_a b_c}{2.303(b_a + b_c)} * \frac{1}{R_p} = \frac{B}{R_p} \quad (8)$$

where  $b_a$  represents the anodic side of Tafel slope (mV decade<sup>-1</sup>),  $b_c$  the cathodic side of Tafel slope (mV decade<sup>-1</sup>),  $B$  the systematic coefficient called Stern-Geary constant (mV) and  $R_p$  the LPR ( $\Omega$  cm<sup>2</sup>).

The Stern-Geary constant was determined from separate Tafel measurements at  $[Cl^-] = 0.7, 1.5, 3$  and  $5$  M as well as  $T = 27, 65$  and  $90$  °C.  $B$  varied from 17.2 to 30.0 mV in resulting in Eq. (9) for determining the  $B$  value. In Eq. (9) temperature is in degrees centigrade and concentration in mol dm<sup>-3</sup>. Results outside of studied range (i.e., temperatures below 27 and above 90 °C) were extrapolated.

$$B = 8.00 + 0.14T + 1.89[Cl^-] \quad (9)$$

The Levich equation (Eq. (10)) applies to totally mass-transfer limited conditions and predicts that the diffusion-limited cathodic current is proportional to the oxidant concentration in bulk solution and to the square root of rotational speed (Bard and Faulkner, 1980). Levich plot showing reaction rate as the function of the square root of angular speed,  $i_{lim,c}$  vs.  $\omega_{rad}^{1/2}$ , is a procedure to determine the rate-limiting step (Jeffrey et al., 2001). A linear dependency of these variables suggests that gold dissolution is limited by diffusion of oxidant (Jeffrey et al., 2001). Bard and Faulkner (1980) emphasized that the linearity is not the only requirement, but the  $i_{lim,c}$  vs.  $\omega_{rad}^{1/2}$  should also intersect the origin. If the relation is not linear or the plot does not intersect the origin, the limiting step is electron transfer rather than the diffusion of oxidant (Jeffrey et al., 2001). Moreover, Angelidis et al. (1993) suggested that if the relation of the leaching rate and the square root of rotational speed is first linear at lower rotational speeds, but then changes at higher rotational speeds, then mass transfer as a rate-controlling step has changed to chemical or mixed control.

$$i_{lim,c} = -0.620zFAD_0^{2/3} \omega_{rad}^{1/2} \nu^{-1/6} C_0^* \quad (10)$$

where  $i_{lim,c}$  is the diffusion-limited cathodic current (mA cm<sup>-2</sup>),  $z$  the number of transferred electrons during reaction,  $F$  is Faraday's constant (96,485 C mol<sup>-1</sup>),  $A$  the area of the electrode (cm<sup>2</sup>),  $D_0$  the diffusion coefficient of oxidant (cm<sup>2</sup> s<sup>-1</sup>),  $\omega_{rad}$  the angular speed (rad s<sup>-1</sup>),  $\nu$  the kinematic viscosity (cm<sup>2</sup> s<sup>-1</sup>) and  $C_0^*$  the concentration of oxidant in bulk solution (mol cm<sup>-3</sup>).

Levich plot showing reaction rate as the function of the square root of angular speed,  $i_{lim,c}$  vs.  $\omega_{rad}^{1/2}$ , is a procedure to determine the rate-limiting step (Jeffrey et al., 2001). A linear dependency of these variables suggests that gold dissolution is limited by diffusion of oxidant (Jeffrey et al., 2001). Bard and Faulkner (1980) emphasized that the linearity is not the only requirement, but the  $i_{lim,c}$  vs.  $\omega_{rad}^{1/2}$  should also intersect the origin. If the relation is not linear or the plot does not intersect the origin, the limiting step is electron transfer rather than the diffusion of oxidant (Jeffrey et al., 2001). Moreover, Angelidis et al. (1993) suggested that if the relation of the leaching rate and the square root of rotational speed is first linear at lower rotational speeds, but then changes at higher rotational speeds, then mass transfer as a rate-controlling step has changed to chemical or mixed control.

If both diffusion and the chemical reaction are limiting the reaction rate, the Koutecký-Levich equation (Eq. (11)) then applies (Bard and Faulkner, 1980):

$$\frac{1}{i} = \frac{1}{i_K} + \frac{1}{i_{lim,c}} = \frac{1}{i_K} + \frac{1}{0.620zFAC_O^*D_O^{2/3}\nu^{-1/6}\omega^{1/2}} \quad (11)$$

where  $i$  represents the sum of the currents due to electron transfer and diffusion,  $i_K$  the electron transfer limited current ( $\text{mA cm}^{-2}$ ) and  $i_{lim,c}$  the mass transfer limited current of cathodic reaction ( $\text{mA cm}^{-2}$ ).

Additionally, Arrhenius equation can be used to calculate the activation energy, the value being indicative of the rate limiting step, Eq. (12) (Peters, 1973). Further, error limit of activation energy can be determined as the error of linear regression slope.

$$k = Ae^{-E_aRT^{-1}} \quad (12)$$

where  $k$  is the rate constant,  $A$  the frequency factor,  $E_a$  the activation energy ( $\text{J mol}^{-1}$ ),  $R$  the universal gas constant ( $8.314 \text{ J mol}^{-1} \text{ K}^{-1}$ ) and  $T$  the temperature (K).

## 2.4. Modeling methods

Gold is dissolved from the rotating gold disc electrode due to oxidation reaction of gold in chloride solution by the oxidant ( $\text{Fe}^{3+}$ ) at the surface of the disc. It is assumed that gold surface reaction rate ( $r_s$ ) can be described by a simple rate equation (Eq. (13)):

$$r_s = k(c_{\text{Fe}^{3+,s}})^{n_1}(c_{\text{Cl}^-,\text{blk}})^{n_2} \quad (13)$$

where  $c_{\text{Fe}^{3+,s}}$  is the concentration of the oxidant at the disc surface,  $c_{\text{Cl}^-,\text{blk}}$  the chloride ion concentration at liquid bulk phase and  $n_1$  and  $n_2$  the reaction orders. Since  $[\text{Cl}^-]$  was always in excess to  $[\text{Fe}^{3+}]$ , it is assumed that  $\text{Cl}^-$  bulk phase concentration can be used. This is justified assumption when considering relatively high chloride concentrations (2–4 M) compared to ferric ion concentrations (0.01–0.5 M). Furthermore, Jeffrey et al., (2001) presented that at high chloride concentration the dissolution rate is ultimately limited by the diffusion of oxidant.

The temperature dependence of the rate constant ( $k$ ) is taken into account by the Arrhenius equation (Eq. (14)) given in a parameterised form as:

$$k = k_{mean} \left( E_a \left( \frac{1}{T} - \frac{1}{T_{mean}} \right) \right) \quad (14)$$

where  $T_{mean}$  is a reference temperature (K) and  $k_{mean}$  the rate constant at the reference temperature.

One possibility is that the dissolution rate could be described as a mixed-control mechanism, where both the surface reaction and diffusion affect gold dissolution rate. The oxidant ( $\text{Fe}^{3+}$ ) diffuses through a boundary layer to the disc surface. Mass transfer of the oxidant through the boundary layer can be described by Eq. (15):

$$\dot{n}_{\text{Fe}^{3+}} = k_L(c_{\text{Fe}^{3+},\text{blk}} - c_{\text{Fe}^{3+,s}}) \quad (15)$$

where  $k_L$  is the mass transfer coefficient through the boundary layer and  $c_{\text{Fe}^{3+},\text{blk}}$  the concentration of oxidant in the liquid bulk phase. At steady state,  $r_s = \gamma \dot{n}_{\text{Fe}^{3+}}$ , and  $c_{\text{Fe}^{3+,s}}$  can be solved iteratively from Eqs. (13) and (15).  $\gamma$  is the stoichiometric coefficient of  $\text{Fe}^{3+}$  to oxidize 1 mol of gold.

Mass transfer to the surface of a rotating disc has been studied by several authors (Sulaymon and Abbar, 2012; Petrescu et al., 2009; Dib and Makhoulouf, 2007). The mass transfer correlation has the general form (Eq. (16)):

$$Sh = a_1 Re^{a_2} Sc^{1/3} \quad (16)$$

where the  $Sh$  is the Sherwood number,  $Re$  the Reynolds number,  $a_1$  the constant in general mass transfer correlation,  $a_2$  the fitted exponent for the Reynolds number and  $Sc$  the Schmidt number. The Sherwood number is defined as (Eq. (17)):

$$Sh = \frac{k_L d}{D} \quad (17)$$

where  $d$  is the rotating disc diameter, and  $D$  is the diffusion coefficient.

The Reynolds number is defined as (Eq. (18)):

$$Re = \frac{\omega_{cyc} d^2}{\nu} \quad (18)$$

where  $\nu$  is the kinematic viscosity.

The Schmidt number is defined as (Eq. (19)):

$$Sc = \frac{\nu}{D} \quad (19)$$

Both, the diffusion coefficient and the kinematic viscosity depend on temperature, which needs to be taken into account when calculating the mass transfer coefficient.

The diffusion coefficient of  $\text{Fe}^{3+}$  in electrolyte solutions has been discussed by Gil et al., (1996) and the value reported is  $4.8 \cdot 10^{-9} \text{ m}^2 \text{ s}^{-1}$  at  $26 \text{ }^\circ\text{C}$  in 1 M  $\text{H}_2\text{SO}_4$  solution. Correction to other temperatures can be done by using the Stokes-Einstein relation (Eq. (20)).

$$\left( \frac{D^0 \mu^0}{T} \right)_{T_1} = \left( \frac{D^0 \mu^0}{T} \right)_{T_2} \quad (20)$$

where  $D$  is the diffusion coefficient of  $\text{Fe}^{3+}$  and  $\mu$  is the dynamic viscosity.

The gold dissolution rate model composed of Eqs. (13)–(17) has 6 parameters,  $k_{1,mean}$ ,  $E_a$ ,  $n_1$ ,  $n_2$ ,  $a_1$ , and  $a_2$ . These parameters were estimated by comparing the calculated gold dissolution rates to the measured rates from the RDE experiments. In the solution of the model, the surface concentration of the oxidant  $c_{\text{Fe}^{3+,s}}$  was solved iteratively from the balance between Eqs. (13) and (15). The model parameters were estimated using the Modest software (Haario, 2002).

The model parameters were first estimated with standard least squares fitting by minimizing the squared difference between the measured and the calculated gold leaching rates. The goodness of the fit was determined by the  $R^2$  value and the standard errors from the estimation. However, to thoroughly evaluate the accuracy and reliability of the estimated parameters in a nonlinear multiparameter model, it is important also to consider possible cross-correlation and identifiability of the parameters. Classical statistical analysis that gives the optimal parameter values, their error estimates, and correlations between them, is based on linearization of the model and is, therefore, approximate. Furthermore, it may sometimes even be quite misleading, especially if the available data are limited and the parameters are poorly identified. The importance of parameter reliability evaluation in development of leaching processes has been stressed (Baldwin and Demopoulos, 1998; Lampinen, 2016). The reliability of the models and their parameters was investigated in this study using the Markov chain Monte Carlo (MCMC) method. The MCMC method is based on Bayesian inference and gives the probability distribution of solutions. MCMC methods have recently been successfully applied in various modeling cases to study parameter reliability (Kuosa et al., 2009; Lampinen et al., 2015b; Vahteristo et al., 2013; Zhukov et al., 2017).

Moreover, the question of the reliability of the model predictions remains unaddressed, i.e., how the uncertainty in the model parameters is reflected in the model response. According to a Bayesian paradigm all the parametrizations of the model that statistically fit the data equally well are determined. The distribution of the unknown parameters is generated using available prior information (e.g., results obtained from previous studies or bound constraints for the parameters) and statistical knowledge of the observation noise. Computationally, the distribution is generated using the MCMC sampling approach. The length of the calculated chain was 200,000 samples. Simple flat, uninformative priors with minimum and maximum bounds set for each parameter were used in the calculation of the chain. Up-to-date adaptive computational schemes are employed in order to make the simulations as effective as possible (Haario et al., 2001; Laine, 2008). In this study, a FORTRAN 90 software package, MODEST 15 (Haario, 2002), was used for both the least-squares and the MCMC estimation. The two methods

are also implemented in a MATLAB package (Laine, 2008; Laine, 2013).

### 3. Results and discussion

#### 3.1. Effect of process variables

First, the effect of temperature on gold dissolution rate was determined by RDE at  $T = 25\text{--}95\text{ }^\circ\text{C}$ ,  $\omega_{\text{cyc}} = 100\text{--}2500\text{ RPM}$ ,  $[\text{Fe}^{3+}] = 0.5\text{ M}$ ,  $[\text{Cl}^-] = 3\text{ M}$  and  $\text{pH} = 1.0$  (Fig. 1). Changes in  $R_p$  were shown to be most significant between  $\omega_{\text{cyc}}$  values of 100 and 300 RPM, whereas smaller change was observed at rotational speeds  $> 1000\text{ RPM}$ . As a consequence, gold dissolution rate increased with increasing rotational speed at all temperatures. Additionally, increase in temperature was shown to increase gold dissolution in ferric chloride solution. This is in line with Liu and Nicol (2002), who also found increasing temperature promotes the anodic dissolution of gold in ferric chloride leaching.

Fig. 2 presents the effect of pH on the gold dissolution rate. pH values 0 and 0.5 both were shown to result in higher gold dissolution rate compared to those observed at pH 1.0. However, the difference in gold dissolution rates was minimal, which suggests that dissolution rate did not have a clear dependency on pH range  $\text{pH} = 0\text{--}1.0$ . pH lower than 1.5 is recommended in gold ferric chloride leaching, as iron started to precipitate at  $95\text{ }^\circ\text{C}$  ( $[\text{Fe}^{3+}] = 0.5\text{ M}$  and  $[\text{Cl}^-] = 3\text{ M}$ ) at  $\text{pH} = 1.5$ . Values higher than 1.5 in gold dissolution can be justified if very low oxidant (ferric ion) concentrations are used for oxidation, i.e. pH controlling the oxidant (ferric species) concentration level in the solution.

Fig. 3 shows the effect of ferric ion concentration on gold dissolution rate. The dissolution of gold increased with increase in ferric ion concentration up to  $[\text{Fe}^{3+}] = 0.75\text{ M}$ , however, the dissolution rates at 0.5 to 1 M were almost the same. It can be stated that gold dissolution increased with increasing ferric concentration up to 0.5 M, after which it did not increase significantly.

Fig. 4 presents the effect of chloride concentration on the gold dissolution rate. The dissolution rates were calculated from  $R_p$  values by Eq. (8), when systematic coefficient ( $B$ ) was either 25.2 mV ( $[\text{Cl}^-] = 2\text{ M}$ ), 27.1 mV ( $[\text{Cl}^-] = 3\text{ M}$ ), 29.0 mV ( $[\text{Cl}^-] = 4\text{ M}$ ) or 30.9 mV ( $[\text{Cl}^-] = 5\text{ M}$ ) with the standard error of  $\pm 3.1\text{ mV}$  for each value. The dissolution rate of gold was shown to increase at all rotational rates with increasing chloride concentration increased up to  $[\text{Cl}^-] = 4\text{ M}$ . However, the dissolution rate of gold decreased, when chloride concentration increased from 4 to 5 M.

#### 3.2. Redox potential of the electrolyte

In order to compare the theoretical redox potential of the solution to the measured potential, Eq. (23) was applied. Equilibrium potentials were calculated with HSC 8.1 (HSC 8.1, 2015) and with Nernst equation: Eq. (21) for the anodic oxidation of  $\text{AuCl}_2^-$  into  $\text{AuCl}_4^-$ , Eq. (22) for the anodic oxidation of Au into  $\text{AuCl}_2^-$  or  $\text{AuCl}_4^-$  and Eq. (23) for the cathodic reduction of  $\text{Fe}^{3+}$  into  $\text{Fe}^{2+}$ .

$$E = E^0 - \frac{RT}{zF} \ln \frac{[\text{AuCl}_2^-] \cdot [\text{Cl}^-]^2}{[\text{AuCl}_4^-]} \quad (21)$$

$$E = E^0 - \frac{RT}{zF} \ln \frac{[\text{Cl}^-]^x}{[\text{AuCl}_x^-]} \quad (22)$$

$$E = E^0 - \frac{RT}{zF} \ln \frac{[\text{Fe}^{2+}]}{[\text{Fe}^{3+}]} \quad (23)$$

where  $E^0$  is the standard equilibrium potential (V) determined by HSC 8.1,  $T$  the temperature (K),  $[\text{AuCl}_2^-]$  and  $[\text{AuCl}_4^-]$  the concentration of  $\text{AuCl}_2^-$  and  $\text{AuCl}_4^-$ ,  $[\text{AuCl}_x^-]$  the concentration of  $\text{AuCl}_2^-$  or  $\text{AuCl}_4^-$ ,  $x$  the number of chloride ions involved in reaction,  $[\text{Cl}^-]$  the concentration of free chlorides,  $[\text{Fe}^{2+}]$  the concentration of ferrous ions as well as  $[\text{Fe}^{3+}]$  the concentration of ferric ions. However, it should be

noted that Eq. (23) is valid, when ferric ions are present in solution as  $\text{Fe}^{3+}$ , not in chloro complexes. This simple form of Nernst equation can be used, since  $\text{Fe}^{3+}$  ions are predominant with chloride concentration from 0 to 2 M (Strahm et al., 1979).

Fig. 5 presents the measured redox potential (0.694–0.740 V vs. SCE) as a function of the logarithm of the ferric iron concentration. Increase in ferric iron concentration was shown to increase solution redox potential.

In order to determine the dependency between gold dissolution behavior and chloride concentration, redox potential was first investigated. Fig. 6 shows that in ferric chloride solution redox potential decreased from 741 to 704 mV vs. SCE as chloride concentration increased from 2 to 5 M, when  $[\text{Fe}^{3+}] = 0.5\text{ M}$ ,  $T = 95\text{ }^\circ\text{C}$  and  $\text{pH} = 1.0$ . However, Fig. 4 shows that the dissolution rate increased when chloride concentration increased from 2 to 4 M. Therefore, it is clear that redox potential does not alone determine the kinetics of gold dissolution. When chloride concentration increased the OCPs were shown to decrease, while dissolution rates of gold increased. Therefore, according to mixed potential theory, the rate of anodic reaction, in this case gold dissolution, increased (Stern and Geary, 1957).

Increase in temperature increased measured redox potential, Fig. 7. The values of measured redox potentials (0.636–0.726 V vs. SCE) did not correspond to the potentials calculated with the Nernst equation (Eq. (23)): 0.807–0.958 V vs. SCE with the lowest ferrous concentration (i.e.  $8.4 \cdot 10^{-8}\text{ M}$ ) and 0.670–0.789 V vs. SCE with the highest ferrous concentration (i.e.  $1.6 \cdot 10^{-5}\text{ M}$ ). With  $[\text{Fe}^{2+}] = 7 \cdot 10^{-5}\text{ M}$ , the calculated and measured redox potentials were almost similar (0.631–0.742 V vs. SCE), but ferrous concentration was calculated to vary between  $8.4 \cdot 10^{-8}\text{ M}$  and  $1.6 \cdot 10^{-5}\text{ M}$  in experiments with the assumption that ferric ions would react only into ferrous ions. However, it should be noted that ferric ions occurs also as chloro complexes in ferric chloride solution. Comparison of measured and calculated redox potentials is presented in Fig. 8.

The increase in ferric iron concentration as well as redox potential correlated with increase in gold dissolution rate up to ca.  $E_{\text{redox}} = 0.73\text{ V}$  vs. SCE, Fig. 9. It should be noted that though redox potential increased linearly with ferric iron concentration (see Fig. 5), gold dissolution rate did not increase significantly, when exceeding  $[\text{Fe}^{3+}] = 0.5\text{ M}$  and redox potential of 0.72 V vs. SCE (see Figs. 3 and 9).

Redox potential was found to vary between 636 and 741 mV vs. SCE in all the experiments. An increase in temperature and ferric concentration increased, but increasing chloride concentration decreased redox potential. Corresponding dissolution rates varied from  $3.9 \cdot 10^{-6}\text{ mol m}^{-2}\text{ s}^{-1}$  with redox potential of 636 mV vs. SCE ( $T = 25\text{ }^\circ\text{C}$ ,  $[\text{Fe}^{3+}] = 0.5\text{ M}$ ,  $[\text{Cl}^-] = 3.0\text{ M}$ ,  $\text{pH} = 1.0$  and  $\omega_{\text{cyc}} = 100\text{ RPM}$ ) to  $7.3 \cdot 10^{-4}\text{ mol m}^{-2}\text{ s}^{-1}$  with redox potential of 717 mV vs.

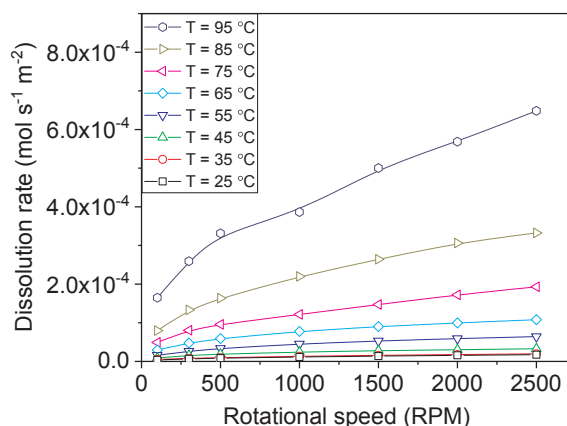


Fig. 1. The gold dissolution rate as a function of rotational speed with  $T = 25\text{--}95\text{ }^\circ\text{C}$ ,  $\omega_{\text{cyc}} = 100\text{--}2500\text{ RPM}$ ,  $[\text{Fe}^{3+}] = 0.5\text{ M}$ ,  $[\text{Cl}^-] = 3.0\text{ M}$  and  $\text{pH} = 1.0$ .

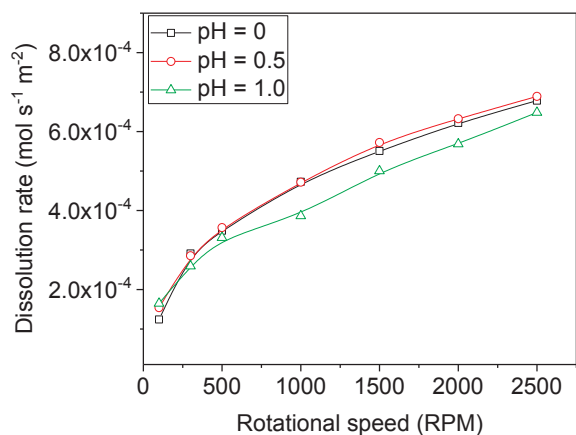


Fig. 2. The effect of pH on the gold dissolution rate as a function of rotational speed, when  $\text{pH} = 0\text{--}1.0$ ,  $\omega_{\text{cyc}} = 100\text{--}2500$  RPM,  $[\text{Fe}^{3+}] = 0.5$  M,  $[\text{Cl}^-] = 3.0$  M and  $T = 95$  °C.

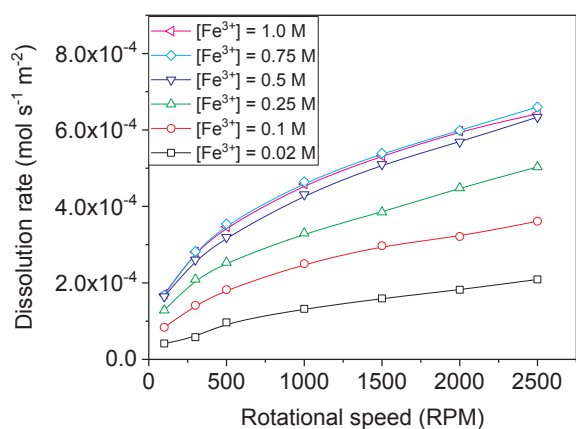


Fig. 3. The effect of ferric concentration on the gold dissolution rate as a function of rotational speed, when  $[\text{Fe}^{3+}] = 0.02\text{--}1$  M,  $\omega_{\text{cyc}} = 100\text{--}2500$  RPM,  $[\text{Cl}^-] = 3.0$  M,  $T = 95$  °C and  $\text{pH} = 1.0$ .

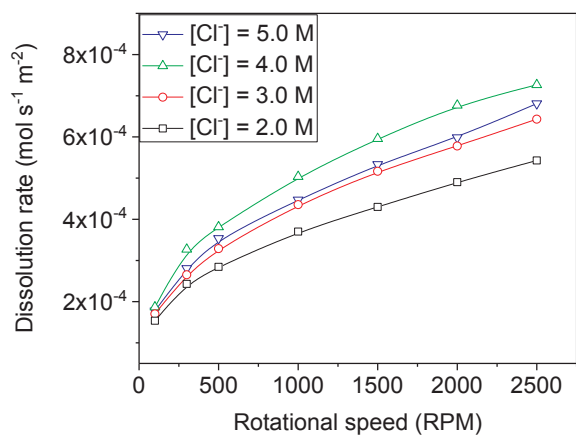


Fig. 4. The effect of chloride concentration on the gold dissolution rate as a function of rotational speed, when  $[\text{Cl}^-] = 2\text{--}5$  M,  $\omega_{\text{cyc}} = 100\text{--}2500$  RPM,  $[\text{Fe}^{3+}] = 0.5$  M,  $T = 95$  °C and  $\text{pH} = 1.0$ .

SCE ( $T = 95$  °C,  $[\text{Fe}^{3+}] = 0.5$  M,  $[\text{Cl}^-] = 4$  M,  $\text{pH} = 1.0$  and  $\omega_{\text{cyc}} = 2500$  RPM). However, with the highest redox potential (741 mV vs. SCE), gold dissolution rate was  $5.4 \cdot 10^{-4} \text{ mol m}^{-2} \text{ s}^{-1}$  ( $T = 95$  °C,  $[\text{Fe}^{3+}] = 0.5$  M,  $[\text{Cl}^-] = 2$  M,  $\text{pH} = 1.0$  and  $\omega_{\text{cyc}} = 2500$  RPM). Therefore, it can be concluded that redox potential affects linearly gold dissolution rate up to approximately 0.73 V (corresponding to  $[\text{Fe}^{3+}] = 0.75$  M), Fig. 9.

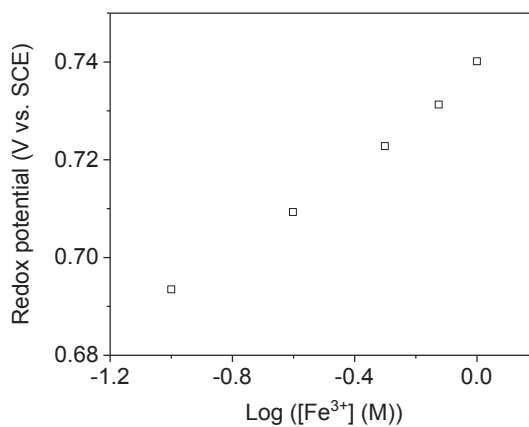


Fig. 5. Redox potential as a function of logarithm of ferric iron concentration, when  $[\text{Fe}^{3+}] = 0.1\text{--}1$  M,  $[\text{Cl}^-] = 3$  M,  $T = 95$  °C and  $\text{pH} = 1.0$ .

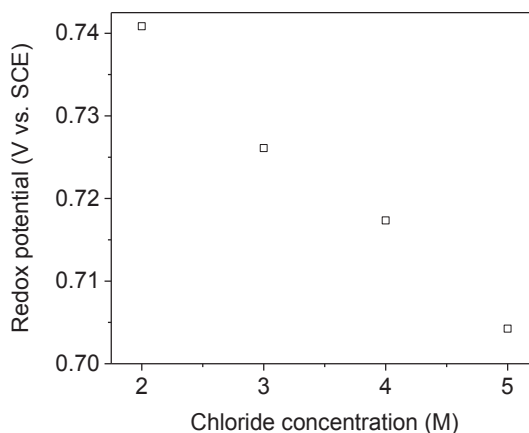


Fig. 6. Redox potential as a function chloride concentration, when  $[\text{Cl}^-] = 2\text{--}5$  M,  $[\text{Fe}^{3+}] = 0.5$  M,  $T = 95$  °C and  $\text{pH} = 1.0$ .

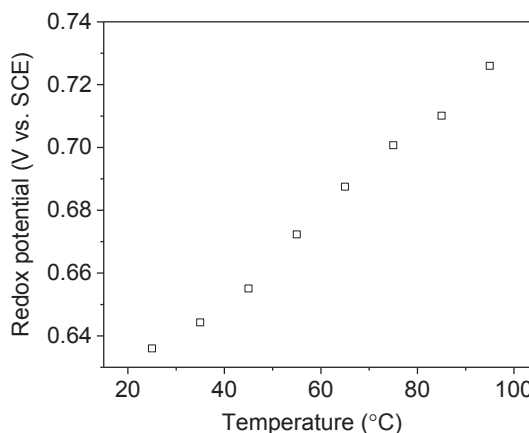


Fig. 7. Measured redox potential of the gold leaching solution as a function of temperature prior to gold exposure into the solution,  $T = 25\text{--}95$  °C,  $[\text{Fe}^{3+}] = 0.5$  M,  $[\text{Cl}^-] = 3$  M and  $\text{pH} = 1.0$ .

The decreasing gold dissolution rate, when chloride concentration increased from 4 to 5 M as well as ferric concentration increased from 0.75 to 1.0 M, is in line with Liu and Nicol (2002). The anodic reaction rates increased with increasing chloride concentration, but the rate of cathodic reaction (reduction of ferric ions) decreased with increase in chloride concentration (Liu and Nicol, 2002). The anodic dissolution is rate-determining step at 2–4 M, but cathodic reaction becomes limiting at higher chloride concentrations.

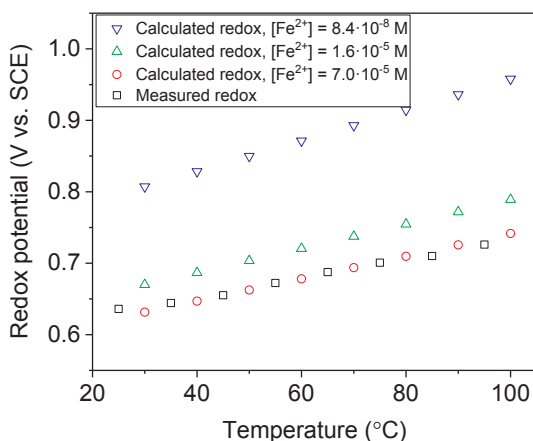


Fig. 8. Measured redox potential at  $T = 25\text{--}95\text{ }^\circ\text{C}$ ,  $[\text{Fe}^{3+}] = 0.5\text{ M}$ ,  $[\text{Cl}^-] = 3\text{ M}$  and  $\text{pH} = 1.0$  and calculated redox potentials at  $T = 20\text{--}100\text{ }^\circ\text{C}$ ,  $[\text{Fe}^{3+}] = 0.5\text{ M}$  and  $[\text{Fe}^{2+}] = 8.4 \cdot 10^{-8}/1.6 \cdot 10^{-5}/7.0 \cdot 10^{-5}\text{ M}$ .

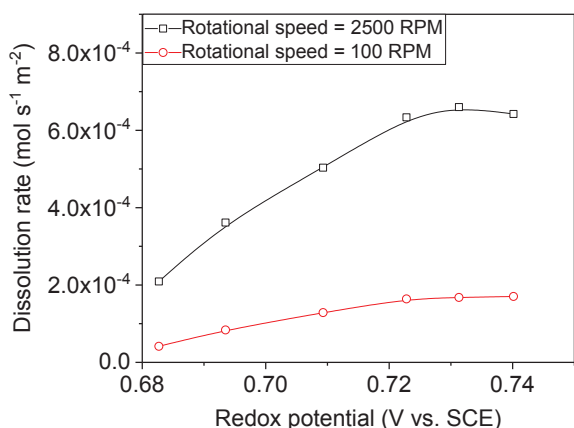


Fig. 9. The dissolution rate of gold as a function of redox potential, when  $\omega_{\text{cyc}} = 100\text{--}2500\text{ RPM}$ ,  $[\text{Fe}^{3+}] = 0.02\text{--}1\text{ M}$ ,  $[\text{Cl}^-] = 3\text{ M}$ ,  $T = 95\text{ }^\circ\text{C}$  and  $\text{pH} = 1.0$ .

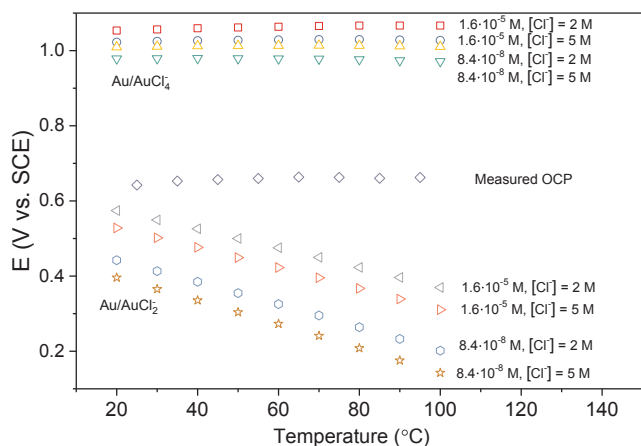


Fig. 10. Equilibrium potential of  $\text{Au}/\text{AuCl}_2^-$  and  $\text{Au}/\text{AuCl}_4^-$  in solution with  $[\text{Cl}^-] = 2\text{--}5\text{ M}$  and  $[\text{Au}^+/\text{Au}^{3+}] = 1.6 \cdot 10^{-5}\text{--}8.4 \cdot 10^{-8}\text{ M}$  at  $T = 20\text{--}100\text{ }^\circ\text{C}$  as a function of temperature.  $E^0$  values are calculated by HSC 8.1 and equilibrium potentials with Nernst equation, and they are compared to the measured OCPs, when  $T = 25\text{--}95\text{ }^\circ\text{C}$ ,  $[\text{Fe}^{3+}] = 0.5\text{ M}$ ,  $[\text{Cl}^-] = 3\text{ M}$  and  $\text{pH} = 1.0$ .

### 3.3. Oxidation state of gold

In the current research, the OCP varied from 597 to 684 mV vs. SCE at investigated ferric concentrations (0.02–1 M). During RDE experiments the OCP was shown to vary from 642 to 662 mV vs. SCE, at

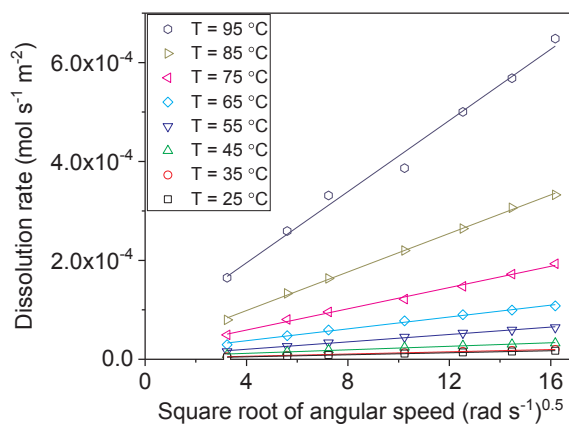


Fig. 11. The Levich plot presents the dissolution rate of gold as a function of  $\omega_{\text{rad}}^{0.5}$ , when  $T = 25\text{--}95\text{ }^\circ\text{C}$ ,  $\omega_{\text{cyc}} = 100\text{--}2500\text{ RPM}$  corresponding  $\omega_{\text{rad}} = 10.5\text{--}262\text{ rad s}^{-1}$ ,  $[\text{Fe}^{3+}] = 0.5\text{ M}$ ,  $[\text{Cl}^-] = 3.0\text{ M}$  and  $\text{pH} = 1.0$ .

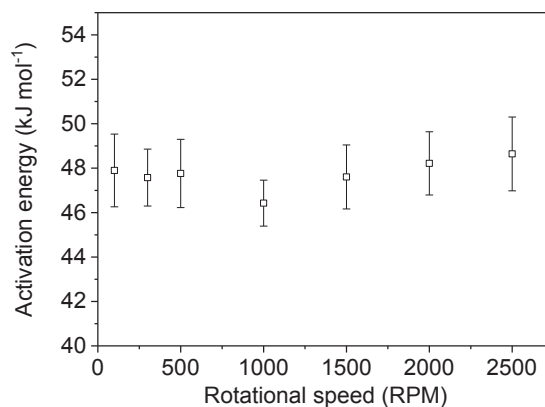


Fig. 12. The activation energy as a function of rotational speed, the error limits defined as the errors of linear regression slope, when  $T = 35\text{--}95\text{ }^\circ\text{C}$ ,  $\omega_{\text{cyc}} = 100\text{--}2500\text{ RPM}$ ,  $[\text{Fe}^{3+}] = 0.5\text{ M}$ ,  $[\text{Cl}^-] = 3.0\text{ M}$  and  $\text{pH} = 1.0$ .

investigated temperatures (25–95 °C), Fig. 10. The highest gold dissolution rate was achieved with the rotational speed of 2500 RPM, when  $[\text{Fe}^{3+}] = 0.5\text{ M}$ ,  $[\text{Cl}^-] = 4\text{ M}$ ,  $T = 95\text{ }^\circ\text{C}$  and  $\text{pH} = 1.0$ , whereas the lowest with the rotational speed of 100 RPM, when  $[\text{Fe}^{3+}] = 0.5\text{ M}$ ,  $[\text{Cl}^-] = 3\text{ M}$ ,  $T = 25\text{ }^\circ\text{C}$  and  $\text{pH} = 1.0$ . The equilibrium potentials calculated with Eq. (22) for  $\text{Au}/\text{AuCl}_2^-$  varied from 143 to 574 mV, while the equilibrium potential for  $\text{Au}/\text{AuCl}_4^-$  varied from 971 to 1067 mV, Fig. 10. Rotational speed did not affect OCP value, though dissolution rates of gold increased, when rotational speed increased. Therefore, it can be stated that increasing mass transfer rate promotes equally both anodic and cathodic reactions.

Fig. 10 shows that the calculated equilibrium potential of  $\text{Au}/\text{AuCl}_4^-$  did not vary significantly with increasing temperature but remains close to 1.0 V vs. SCE, however, the equilibrium potential of  $\text{Au}/\text{AuCl}_2^-$  was shown to decrease with increasing temperature. Despite the temperature, measured OCPs were always higher than equilibrium potentials of  $\text{Au}/\text{AuCl}_2^-$ , but lower than equilibrium potentials of  $\text{Au}/\text{AuCl}_4^-$ . However, OCPs more close to equilibrium potentials of  $\text{Au}/\text{AuCl}_2^-$  suggested that the gold oxidation state of +1 was predominant in the investigated ferric chloride environment. These results were in line with determined potentials, in which Au occurs as  $\text{AuCl}_2^-$  and  $\text{AuCl}_4^-$ :  $\text{AuCl}_2^- < 0.8\text{ V vs. SCE}$ ,  $\text{AuCl}_4^- > 0.8\text{ V}$  (Diaz et al., 1993),  $\text{AuCl}_2^- < 0.956\text{ V vs. SCE}$ ,  $\text{AuCl}_4^- > 0.956\text{ V}$  (Nicol, 1980) and  $\text{AuCl}_2^- < 0.8\text{ V vs. SCE}$ , while  $\text{AuCl}_4^- > 1.1\text{ V vs. SCE}$  (Frankenthal and Siconolfi, 1982). The determined equilibrium potentials of  $\text{Au}/\text{AuCl}_2^-$  and  $\text{Au}/\text{AuCl}_4^-$  in this study were most similar to Frankenthal and Siconolfi (1982) results.

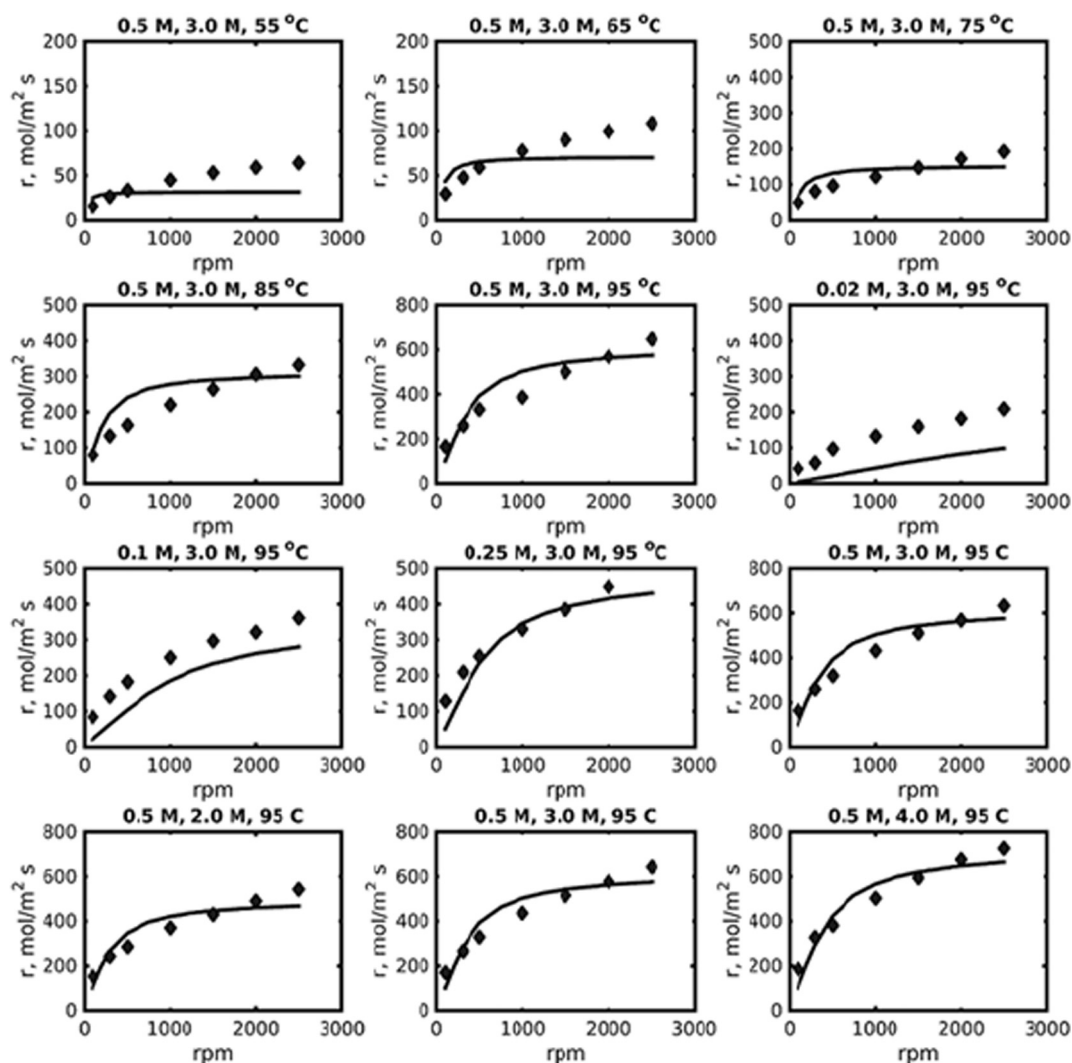


Fig. 13. Comparison of the measured and predicted gold dissolution rates.

For the electrochemical oxidation reaction from  $\text{AuCl}_2^-$  to  $\text{AuCl}_4^-$ , Eq. (6), the calculated equilibrium potential ( $E$ ) (Eq. (21)) at  $T = 25\text{--}95\text{ }^\circ\text{C}$ , varied from 1.25 V ( $[\text{Au}] = 1.6 \cdot 10^{-5}\text{ M}$ ,  $[\text{Cl}^-] = 4\text{ M}$ ,  $T = 25\text{ }^\circ\text{C}$ ) to 1.51 V ( $[\text{Au}] = 8.4 \cdot 10^{-8}\text{ M}$ ,  $[\text{Cl}^-] = 3\text{ M}$ ,  $T = 95\text{ }^\circ\text{C}$ ) vs. SCE. The oxidation of  $\text{AuCl}_2^-$  to  $\text{AuCl}_4^-$  in the studied ferric chloride solutions is thus unlikely.

Thermodynamic calculations using HSC 8.1 software show that the disproportionation reaction (Eq. (4)) has equilibrium constant from  $10^{-13}$  to  $10^{-18}$  at  $T = 0\text{--}100\text{ }^\circ\text{C}$ . Therefore, such disproportionation is not thermodynamically likely to happen. It can be concluded that gold dissolution can be described by Eq. (5) in ferric chloride leaching of gold.

### 3.4. Rate-limiting step of gold dissolution

Fig. 11 presents the gold dissolution rates determined by linear polarization resistance using RDE and Levich plot, when  $T = 25\text{--}95\text{ }^\circ\text{C}$ ,  $\omega_{\text{cyc}} = 100\text{--}2500\text{ RPM}$  corresponding  $\omega_{\text{rad}} = 10.5\text{--}262\text{ rad s}^{-1}$ ,  $[\text{Fe}^{3+}] = 0.5\text{ M}$ ,  $[\text{Cl}^-] = 3.0\text{ M}$  and  $\text{pH} = 1.0$ . The trend lines had high correlation ( $R^2 = 0.985\text{--}0.999$ ), though some scatter occurred at  $T = 95\text{ }^\circ\text{C}$ . However, none of slopes intersected the origin, which indicated that the gold dissolution rate was not purely limited by mass transfer.

Activation energies were calculated ( $T = 35\text{--}95\text{ }^\circ\text{C}$ ,  $\omega_{\text{cyc}} = 100\text{--}2500\text{ RPM}$ ,  $[\text{Fe}^{3+}] = 0.5\text{ M}$ ,  $[\text{Cl}^-] = 3.0\text{ M}$  and  $\text{pH} = 1.0$ ),

were shown to be almost independent of the rotation speed, varying from 46.4 to 48.6  $\text{kJ mol}^{-1}$  with error limits from  $\pm 1.0$  to  $\pm 1.7\text{ kJ mol}^{-1}$ , Fig. 12. These values suggest that gold dissolution reaction was controlled by electron transfer.

### 4. Kinetic model for gold leaching

The activation energy determined by the electrochemical measurements indicated that the gold dissolution rate is limited by the surface reaction. The effect of mass transfer was seen with increasing rotational speed (Figs. 1–4), which indicates that mass transfer also had effect on gold leaching rate. In order to observe the rate limiting steps, a mechanistic model was developed. With mechanistic model rate limiting steps can be separated and their relative importance studied in selected conditions.

The modeling was conducted at ferric ion concentrations from 0.02 to 0.5 M, chloride concentrations from 2 to 4 M, temperature range from 55 to 95  $^\circ\text{C}$  and at  $\text{pH} = 1$ . These conditions can be considered an optimal range for ferric chloride gold leaching, since ferric ion concentration  $> 0.5\text{ M}$  or chloride concentration  $> 4\text{ M}$  was shown not to improve gold dissolution and  $T$  below 55  $^\circ\text{C}$  showed slow dissolution kinetics in the electrochemical experiments. According to the previous discussion about gold leaching chemistry that gold dissolves as described in Eq. (5), a value of 1 is used for  $\gamma$ .

Comparison of the measured and calculated gold dissolution rates is

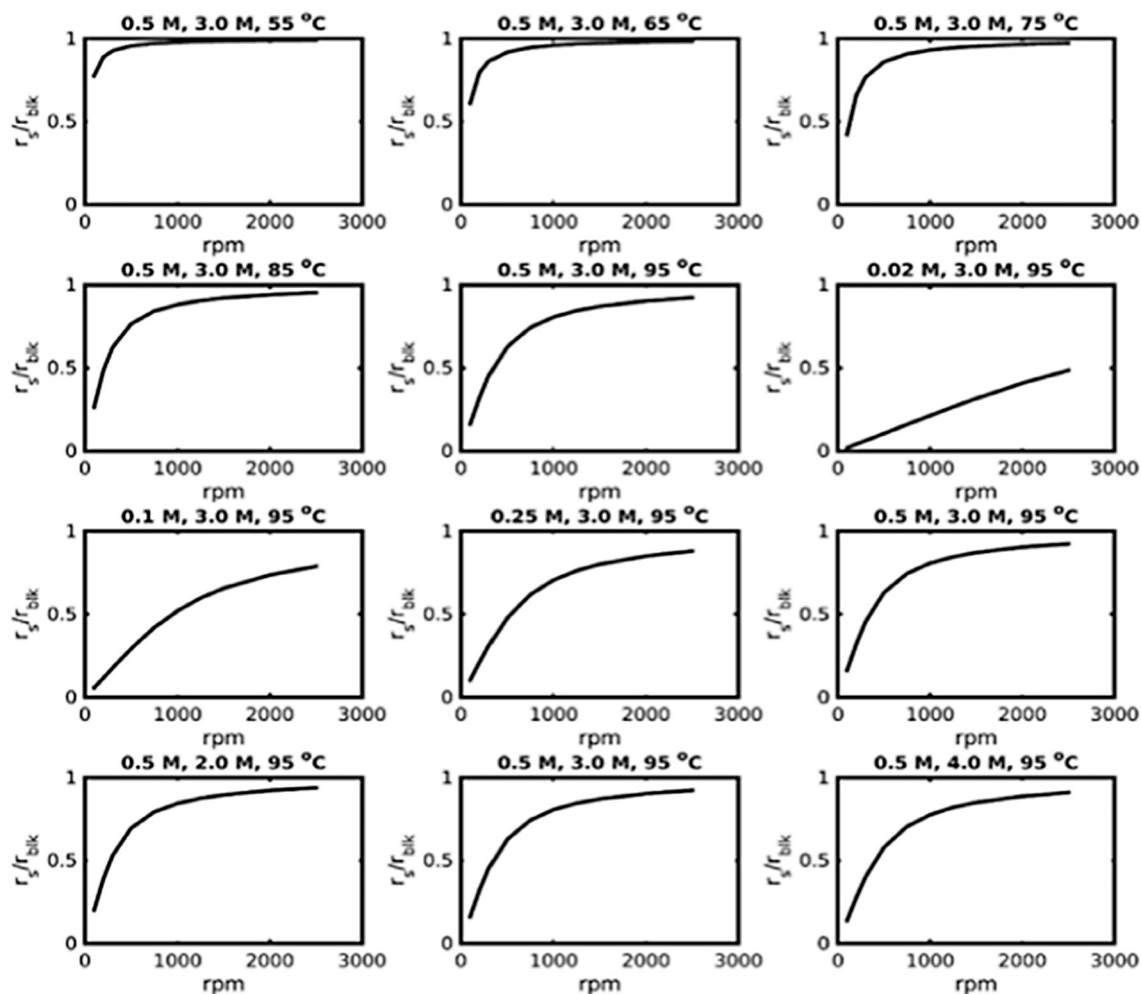


Fig. 14. Ratio of the intrinsic surface reaction rate to reaction rate at bulk oxidant concentration.

**Table 1**  
Estimated parameters for the gold dissolution model in the RDE experiments.

Parameter	$R^2 = 92.19\%$	
	Value	std. error, %
$k_{1,mean}, (\text{m}^3 \text{kmol}^{-1})^{n-1} \text{m s}^{-1}$	$154 \cdot 10^{-6}$	14.5
$E_a, \text{J mol}^{-1}$	$74.7 \cdot 10^{+3}$	6.7
$n_1$	0.349	22.8
$n_2$	0.55	18.1
$a_1$	18.0	15.3
$a_2$	1.03	12.5

shown in Fig. 13. The modeled dissolution rate follows the measured points quite closely as the coefficient of regression for the model was 92.19%. The main discrepancy between the measurements and the simulations can be seen at low temperatures (55 and 65 °C) and with low ferric ion concentrations (0.02 and 0.1 M) where the measured dissolution rate is higher than what is obtained by the model.

As presented above, the measured data always showed a dependency from mass transfer even at high rotational speeds. Hence, the relative importance of mass transfer should be studied in detail. The existence and effect of mass transfer limitations can be studied with the established model by the simulated curves presented in Fig. 14, which shows the ratio of the actual leaching rate over the leaching rate without diffusion limitations (leaching agent concentration at the surface equals the bulk leaching agent concentration calculated from the model as presented). If the ratio presented in Fig. 14 is low ( $< 1$ ) it

means that the overall dissolution rate is limited by mass transfer of oxidant from the bulk phase to the gold surface. If, on the other hand, the ratio is close to unity, the dissolution is mainly controlled by the intrinsic surface reaction. Between these two cases, the dissolution rate is affected by both the reaction and mass transfer steps. The model predicts mainly control by intrinsic surface reaction for gold dissolution. As expected, the obtained results show that at low temperatures (55 and 65 °C) rate is limited by the intrinsic surface reaction, while with low oxidant concentration ( $[\text{Fe}^{3+}] = 0.02 \text{ M}$ ) the dissolution is mainly controlled by mass transfer. With low oxidant concentrations, the concentration difference between the bulk liquid phase and the disc surface is so low that the generated mass transfer rate is not enough to maintain high oxidant surface concentration even at high stirring speeds. Therefore, the dissolution rate remains low. At higher rotational speeds ( $> 1000 \text{ RPM}$ ) the ratio approaches 1.0 in most of the experiments, indicating control by intrinsic surface reaction, as shown in Fig. 14.

The estimated parameters are shown below in Table 1. The activation energy ( $E_a$ ) for the intrinsic surface reaction is  $74.7 \text{ kJ mol}^{-1}$  and the reaction order for  $\text{Fe}^{3+}$  is 0.35. It may be noticed from the parameter estimation results that the fitted exponent for the Reynolds number ( $a_2$ ) is much higher than the theoretical value of 0.5 in the Levich correlation (Dib and Makhloufi, 2007). The exact reason for this is not known, but it can be presented that, since the Levich equation was derived for an ideal case, any nonidealities, such as surface non-uniformities, vibrations, or existence of vapour bubbles probably influence the boundary layer at the disc surface generating higher mass

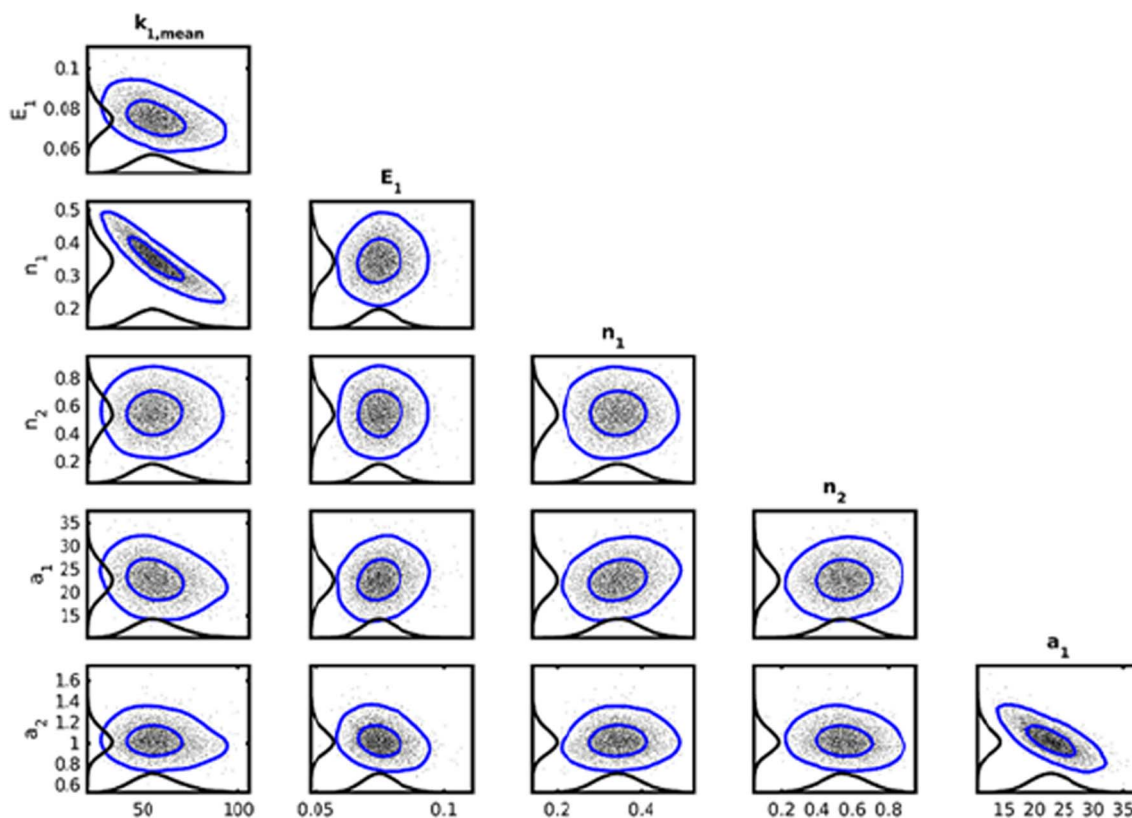


Fig. 15. 2D and 1D marginal posterior distributions for the parameters of the mechanistic model. The lines represent 95% and 50% confidence regions and one dimensional density estimates.

transfer rates than expected compared to the ideal case. Similar behaviour was presented by Lampinen et al. (2017) in gold cupric chloride leaching.

The reliability of the estimated parameters studied by the MCMC method is depicted in Fig. 15 showing the marginal posterior distributions for the estimated parameters. It can be seen that the reliability of the parameters is good. All the distributions are well-centred around the most probable point.

## 5. Conclusions

In this study, the reaction mechanism and kinetics of gold dissolution in ferric chloride solutions were studied with ferric ion concentrations between 0.02 and 1.0 M, chloride concentration between 2 and 5 M, temperature between 25 and 95 °C and pH between 0 and 1.0. The rotating disc electrode (RDE) method was used to measure linear polarization resistance at rotational speeds from 100 to 2500 RPM. According to the calculated equilibrium potentials and measured OCPs, gold dissolved as aurous ion as  $\text{AuCl}_2^-$ , under all test conditions, which is in line with literature. Furthermore, calculated theoretical equilibrium potentials for the oxidation reaction of  $\text{AuCl}_2^-$  to  $\text{AuCl}_4^-$  suggest that this reaction does not occur under the investigated conditions. Additionally, the calculated equilibrium constants suggests that the disproportionation does not occur. The increase in gold dissolution rate was observed to be proportional to increases in temperature, ferric iron concentration as well as the chloride concentration. Further, rotational speed was found not to affect OCP value, though dissolution rates of gold increased, when rotational speed increased in all test conditions. Therefore, it can be concluded that rotational speed promotes equally anodic and cathodic reactions.

OCPs were shown to decrease, while dissolution rates of gold increased, when chloride concentration increased. Therefore, according to mixed potential theory, anodic reaction rate increased. Additionally,

it was shown that the dissolution of gold did not significantly increase when the ferric ion concentration was above 0.5 M. However, the reason for decreasing gold dissolution rate, when chloride concentration increased from 4 to 5 M as well as ferric concentration increased from 0.75 to 1.0 M, was not investigated in this study. pH was shown not to affect clearly on the gold dissolution rate, however, values lower than 1.5 support soluble iron. Redox potential was found to vary between 636 and 741 mV vs. SCE, and temperature and ferric concentration increased redox potential, while increasing chloride concentration was shown to decrease redox potential. The redox potential affected linearly on gold dissolution rate up to approximately 0.73 V vs. SCE (corresponding to  $[\text{Fe}^{3+}] = 0.75 \text{ M}$ ) after which the dissolution rate remained approximately the same.

The reaction mechanism was investigated by the use of Levich plot and by determining activation energies. Levich plot indicated that the gold dissolution rate was not purely limited by mass transfer, though activation energies indicated that the gold dissolution in ferric chloride solution was controlled by the electron transfer. However, the dissolution rates did not reach a constant value with increasing rotational speed of gold RDE at any investigated conditions, therefore, it was expected that mass transfer affects the system regardless of the high rotational speeds.

The rate limiting steps were studied more closely by developing a mechanistic model. With mechanistic model the rate limiting steps were separated and their relative importance studied. The kinetics were modeled in the optimum leaching ranges determined in the current work. The reliability of the mechanistic model and model parameters was investigated in this study using the Markov Chain Monte Carlo (MCMC) method. The model ( $R^2 = 92.19\%$ ) was shown to describe well the leaching data presented and all the estimated model parameters showed good reliability. The model predicted that gold dissolution was mainly controlled by intrinsic surface reaction at rotational speeds > 1000 RPM. At low temperatures (55 and 65 °C) rate

was limited by the intrinsic surface reaction, while with low oxidant concentration ( $[Fe^{3+}] = 0.02 \text{ M}$ ), the dissolution was mainly controlled by mass transfer.

## Acknowledgements

This work was a part of Outotec's AuChloride research project. Therefore, the authors are grateful for Outotec and Tekes for financing this research and for the permission to publish these results. The authors are grateful to Ph.D. Sveta Moiseev for her assistance with the experiments. "RawMatTERS Finland Infrastructure" (RAMI), supported by Academy of Finland, is greatly acknowledged.

## References

- Abe, Y., Hosaka, H., 2010. US 7682420 B2 Method for leaching gold. Nippon Mining & Metals Co. Ltd.
- Adams, M.D., 2016. Chloride as an alternative lixiviant to cyanide for gold ores. In: M.D. Adams (Ed.), *Gold Ore Processing – Project Development and Operations*, vol. 29, pp. 525–534.
- Angelidis, T.N., Kydros, K.N., Matis, K.A., 1993. A fundamental rotating disk study of gold dissolution in ionide-ionide solutions. *Hydrometallurgy* 34, 49–64.
- Aromaa, J., Rintala, L., Kahari, M., Forsen, O., 2014. Dissolution of gold with cyanide replacing reagents. *Physicochem. Probl. Mineral Process.* 51 (1), 269–279.
- Aylmore, M.G., 2005. Alternative lixivants to cyanide for leaching gold ores. In: M.D. Adams (Ed.), *Gold Ore Processing – Project Development and Operations*, vol. 27, pp. 447–484.
- Baldwin, S.A., Demopoulos, G.P., 1998. Parameter sensitivity of kinetics-based hydro-metallurgical reactor models. *Can. J. Chem. Eng.* 76, 1083–1092.
- Bard, A.J., Faulkner, L.R., 1980. *Electrochemical Methods Fundamentals and Applications*, first ed., John Wiley & Sons.
- von Bonsdorff, R., 2006. The use of a quartz crystal microbalance in determining the dissolution rate of gold in cupric chloride solution. Licentiate thesis, first ed. Helsinki University of Technology, Espoo.
- Diaz, M.A., Kelsall, G.H., Welham, H.J., 1993. Electrowinning coupled to gold leaching by electrogenerated chloride: I. Au(III)→Au(I)/Au kinetics in aqueous  $Cl_2/Cl^-$  electrolytes. *J. Electroanal. Chem.* 361, 25–38.
- Dib, A., Makhoulfi, L., 2007. Mass transfer correlation of simultaneous removal by cementation of nickel and cobalt from sulphate industrial solution containing copper Part 1: Onto rotating zinc electrode disc. *Chem. Eng. J.* 130, 39–44.
- Duranceau, S.J., Townley, D., Bell, E.C., 2004. Optimizing corrosion control in water distribution systems, 12–15. Cited at 17.10.2016 from: < [http://www.waterrf.org/ExecutiveSummaryLibrary/90983\\_2648\\_profile.pdf](http://www.waterrf.org/ExecutiveSummaryLibrary/90983_2648_profile.pdf) > .
- Frankenthal, R.P., Siconolfi, D.J., 1982. The anodic corrosion of gold in concentrated chloride solution. *J. Electrochem. Soc.* 129, 1192–1196.
- Gil, A.F., Galicia, L., González, I., 1996. Diffusion coefficients and electrode kinetic parameters of different Fe(III)-sulfate complexes. *J. Electroanal. Chem.* 417, 129–134.
- Haario, H., Saksman, E., Tamminen, J., 2001. An Adaptive Metropolis Algorithm. *Bernoulli* 7, 223–242.
- Haario, H., 2002. *Modest User's Guide*. ProfMath Oy, Helsinki, Finland.
- Hilson, G., Monhemius, A.J., 2006. Alternatives to cyanide in the gold mining industry: prospects for the future? *J. Clean. Prod.* 14, 1158–1167.
- HSC 8.1, 2015. [www.outotec.com](http://www.outotec.com).
- Jeffrey, M.I., Breuer, P.L., Choo, W.L., 2001. A kinetic study that compares the leaching of gold in the cyanide, thiosulfate, and chloride systems. *Metall. Mater. Trans. B* 32 (2), 979–986.
- Kirke Rose, T., 1898. *The metallurgy of gold*. Published: London: C. Griffin; Philadelphia: C. Griffin, 618 p.
- Kuosa, M., Laari, A., Solonen, A., Haario, H., Kallas, J., 2009. Multicomponent reaction kinetics for ozonation of p-nitrophenol and its decomposition products under acidic conditions at constant pH. *Chem. Eng. Sci.* 64, 2332–2342.
- Laine, M., 2008. *Adaptive MCMC Methods with Applications in Environmental and Geophysical Model*. Finnish Meteorological Institute, Helsinki, Finland (Ph.D. Thesis).
- Laine, M., 2013. MCMC toolbox for matlab, 2013. <http://helios.fmi.fi/~lainema/mcmc/> (accessed April 18, 2016).
- Laitos, J.G., 2012. The current status of cyanide regulations. *Eng. Min. J.* 213(2), 34–40. Referred from: < <http://www.e-mj.com/features/1656-the-current-status-of-cyanide-regulations.html#.VrMwLobwmYg> > (19.7.2016).
- Lampinen, M., 2016. Development of hydrometallurgical reactor leaching for recovery of zinc and gold (Ph.D. Thesis). Lappeenranta University of Technology, Finland.
- Lampinen, M., Laari, A., Turunen, I., 2015a. Ammoniacal thiosulfate leaching of pressure oxidized sulphide gold concentrate with low reagent consumption. *Hydrometallurgy* 151, 1–9.
- Lampinen, M., Laari, A., Turunen, I., 2015b. Kinetic model for direct leaching of zinc sulphide concentrates at high and solute concentrations. *Hydrometallurgy* 153, 160–169.
- Lampinen, M., Seisko, S., Forsström, O., Laari, A., Aromaa, J., Lundström, M., Koironen, T., 2017. Mechanism and kinetics of gold leaching by cupric chloride. *Hydrometallurgy* 169, 103–111.
- Liddicoat, J., Dreisinger, 2007. Chloride leaching of chalcopyrite. *Hydrometallurgy* 89 (3–4), 323–331.
- Liu, J.Q., Nicol, M.J., 2002. Thermodynamic and kinetics of the dissolution of gold under pressure oxidation conditions in the presence of chloride. *Can. Metall. Q.* 41 (4), 409–416.
- Lu, J., Dreisinger, D., 2013. Copper leaching from chalcopyrite concentrate in Cu(II)/Fe(III) chloride system. *Miner. Eng.* 45, 185–190.
- Lundström, M., Ahtiainen, R., Haakana, T., O'callaghan, J., 2014. Techno-economical observations related to outotec gold chloride process. In: *Proceedings of Alta 2014*, pp. 89–104.
- Lundström, M., Aromaa, J., Forsén, O., Barker, M.H., 2008. Reaction product layer on chalcopyrite in cupric chloride leaching. *Can. Metall. Q.* 473, 245–252.
- Lundström, M., Aromaa, J., Forsén, O., 2009. Transient surface analysis of dissolving chalcopyrite in cupric chloride solution. *Can. Metall. Q.* 481, 53–60.
- Lundström, M., O'callaghan, J., Haakana, T., Ahtiainen, R., Karonen, J., 2016. WO 2016066905 A1 Process for recovering gold, Outotec (Finland) Oy.
- Marsden, J., House, I., 2006. *The chemistry of gold extraction*. Vol. 2. Littleton (CO), USA: Society of for Mining, Metallurgy and Exploration (SME).
- van Meersbergen, M.T., Lorenzen, L., van Deventer, J.S.J., 1993. The electrochemical dissolution of gold in bromide medium. *Miner. Eng.* 6 (8–10), 1067–1079.
- Nicol, M.J., 1980. The anodic dissolution of gold. Part I. Oxidation in acidic solutions. *Gold Bulletin* 145 (13), 70–75.
- O'Melia, C.R., 1978. Coagulation in waste water treatment. In: K.J. Ives, (Ed.), *The Scientific Basis of Flocculation*. Nato Advanced Study Institute Series, Series E, Applied Science-No. 27. Sijthoff and Noordhoff, Netherlands.
- Muir, D.M., 2002. Basic principles of chloride hydrometallurgy. In: E.M. Peek, G. Van Weert (Eds.), *Chloride Metallurgy 2002*, pp. 759–791.
- Peters, E., 1973. The physical chemistry of hydrometallurgy, in proceeding of international symposium on hydrometallurgy, Chicago, D.J.I. Evans and R.S. Shoemaker, 205–258.
- Petrescu, S., Secula, M.R., Nemțof, G., Grețescu, I., 2009. Study on metal anodic dissolution. *Rev. Chim. (București)* 60, 462–467.
- Potter, R.W., Clynne, M.A., 1980. Solubility of NaCl and KCl in aqueous HCl from 20 to 85 °C. *J. Chem. Eng. Data* 25, 50–51.
- Putnam, G.L., 1944. Chlorine as a solvent in gold hydrometallurgy. *Eng. Min. J.* 145 (3), 70–75.
- Senanayake, G., 2004. Gold leaching in non-cyanide lixiviant systems: critical issues on fundamentals and applications. *Miner. Eng.* 17, 785–801.
- Stern, M., Geary, A.L., 1957. Electrochemical polarization. I. A theoretical analysis of the shape of polarization curves. *J. Electrochem. Soc.* 104 (1), 56–63.
- Strahm, U., Patel, R.C., Matijevic, E., 1979. Thermodynamics and kinetics of aqueous iron (III) chloride complexes formation. *J. Phys. Chem.* 83 (13), 1689–1695.
- Sulaymon, A.H., Abbar, A.H., 2012. Mass transfer to amalgamated copper rotating disc electrode. *J. Electrochem. Sci. Technol.* 3, 165–171.
- UNEP/OCHA, 2000. *Spill of Liquid and Suspended Waste at the Aurul S.A. Retreatment Plant in Baia Mare: Assessment Mission [to] Romania, Hungary, Federal Republic of Yugoslavia*. Report, 57 p.
- Vahteristo, K., Laari, A., Solonen, A., 2013. Diels–Alder reaction kinetics for production of norbornene monomers: evaluation of parameters and model reliability using Markov Chain Monte Carlo Methods. *Ind. Eng. Chem. Res.* 52, 6357–6365.
- Zhukov, V.V., Laari, A., Lampinen, M., Koironen, T., 2017. A mechanistic model for direct pressure leaching of iron containing sphalerite concentrate. *Chem. Eng. Res. Des.* 118, 131–141.